High-Resolution Photoelectron Spectroscopy with Angular Selectivity - A Tool To Probe Valence-Rydberg States and Couplings in HCl+

ARTICLE *in* THE JOURNAL OF PHYSICAL CHEMISTRY A · JUNE 2014

Impact Factor: 2.69 · DOI: 10.1021/jp504505e · Source: PubMed

9 AUTHORS, INCLUDING:

Minna Patanen

University of Oulu

59 PUBLICATIONS **187** CITATIONS

SEE PROFILE

Majdi Hochlaf

Université Paris-Est Marne-la-Vallée

240 PUBLICATIONS **1,592** CITATIONS

SEE PROFILE

John D Bozek

SOLEIL synchrotron

417 PUBLICATIONS **6,825** CITATIONS

SEE PROFILE

Catalin Miron

Horia Hulubei National Institute for R&D in Ph…

158 PUBLICATIONS **1,520** CITATIONS

SEE PROFILE

THE JOURNAL OF PHYSICAL CHEMISTRY A

Article

pubs.acs.org/JPCA

High-Resolution Photoelectron Spectroscopy with Angular Selectivity - A Tool To Probe Valence-Rydberg States and Couplings in HCl^+

M. Patanen,[†] C. Nicolas,[†] R. Linguerri,[‡] G. Simões,[†,§] O. Travnikova,[†] X.-J. Liu,[†] M. Hochlaf,*[,‡] J. D. Bozek,[¶] and C. Miron*[,†]

[†]Synchrotron SOLEIL, L'Orme des Merisiers, Saint-Aubin, BP 48, 91192 Gif-sur-Yvette Cedex, France

[‡]Université Paris-Est, Laboratoire Modélisation et Simulation Multi Echelle, MSME UMR 8208 CNRS, 5 Bd Descartes, 77454 Marne-La-Vallée, France

[¶]SLAC National Accelerator Laboratory 2575 Sand Hill Road, Menlo Park, California 94025, United States

[§]Instituto de Química, Universidade Federal do Rio de Janeiro, Ilha do Fundão, Rio de Janeiro, RJ, Brazil 21949-900

ABSTRACT: Due to strong electron correlation effects and electron coupling with nuclear motion, the molecular inner-valence photoionization is still a challenge in electron spectroscopy, resulting in several interesting phenomena such as drastic changes of angular dependencies, spin−orbit induced predissociation, and complex interplay between adiabatic and nonadiabatic transitions. We investigated the excited electronic states of HCl^+ in the binding energy range 27.5−30.5 eV using synchrotron radiation based high-resolution inner-valence photoelectron spectroscopy with angular resolution and interpreted the observations with the help of *ab initio* calculations. Overlapping electronic states in this region were disentangled through the analysis of photoelectron emission anisotropies. For instance, a puzzling transition, which does not seem to obey either an adiabatic or a nonadiabatic picture, has been identified at ∼28.6 eV binding energy. By this study, we show that ultrahigh-resolution photoelectron spectroscopy with angular selectivity represents a powerful tool to probe the highly excited ionic molecular electronic states and their intricate couplings.

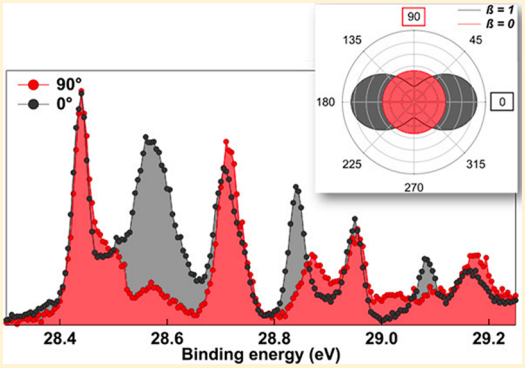

INTRODUCTION

Hydrogen chloride, HCl, is an important molecule involved in the chemistry of the upper atmosphere, thought to be responsible for the depletion of the Antarctic ozone layer through heterogeneous chemical reactions.[1] Very recently, the HCl^+ radical has been observed for the first time in the interstellar medium, where it was shown to be a key intermediate in the chlorine chemistry of the interstellar gas.[2] In addition to being an essential substance in chemistry, and in spite of its apparent simplicity, HCl is also the host of a multitude of fascinating phenomena in chemical physics and quantum mechanics. For instance, an ultrafast neutral dissociation process[3] of Cl 2p core-excited HCl was described by Aksela et al.[4] in the early 1990s, and a continuum-continuum quantum interference between molecular and atomic contributions to the Auger decay was reported by Feifel et al.[5] Also, electronic state interferences were observed in the resonant X-ray emission following Cl K-shell excitation by Kavčič et al.,[6] while strong nonadiabatic transitions in the inner-valence photoelectron spectrum were presented by Burmeister et al.[7,8] Valence photoionization of HCl by an intense near-infrared laser field was used to demonstrate the importance of the excited ionic states contributing to the total and angle-dependent tunnel ionization probability.[9]

Only a few studies of the angularly resolved inner-valence spectrum of HCl have been reported. In 1986, Adam determined the average photoelectron asymmetry parameter β showing a decreasing trend from ≈1.3 to 0.9 for the energy range considered in our study.[10] The resolution achieved in that study did not allow the determination of β for different electronic states separately. Later on, Kukk et al.[11] analyzed the β parameters for the valence ionized states of HCl at nonresonant energy and at several Cl $2p^{-1}nl$ resonances. The β parameter for the electronic states associated with the ionization of the 2π orbital showed strong fluctuations as a function of the initial resonant state, while the β for the electronic states formed by the ejection of a 5σ electron remained almost constant.

In this article we report the angularly resolved inner-valence spectrum of HCl and its interpretation with the support of *ab initio* calculations. In a very narrow energy interval of only 3 eV

Received: May 7, 2014
Revised: June 22, 2014
Published: June 23, 2014

   dx.doi.org/10.1021/jp504505e | *J. Phys. Chem. A* 2014, 118, 4975−4981

we demonstrate the existence of several fascinating phenomena, such as the strong angular dependence of the photoionization cross sections of various electronic states, nonadiabatic transitions in the vicinity of avoided potential curve crossing, and spin−orbit induced predissociations. Calculations revealed some of these phenomena to be associated with highly excited bound states that were not predicted to exist before. In addition, we identified a transition whose β values vary quite strongly from one vibrational substate to another, but thanks to the accurately computed potential energy curves (PECs), we can confidently conclude that all these peaks belong to the same vibrational sequence.

Recently, the vibrationally specific cross sections and photoelectron angular distributions have been shown to strongly deviate from the Franck−Condon behavior close to the photoionization thresholds (see e.g. refs 12 and 13 and references therein) and also in case of resonant photoemission processes, where vibrational scattering anisotropy (VSA) has been recently described[14] even for diatomic molecules.[15] Here we performed our measurements at a photon energy of 100 eV, which is far from any bound or continuum resonant states, excluding the occurrence of the above-mentioned effects. Our present analysis demonstrates that the photoelectron asymmetry parameter β is a useful tool to identify the nature of ionic states within a manifold of overlapping bands.

EXPERIMENTAL SECTION

The experiment was carried out at the PLEIADES beamline,[16−18] at the SOLEIL national synchrotron radiation (SR) facility in Saint-Aubin, France. Out of the two available quasi-periodic undulators, HU256 and HU80, the Apple II − type, permanent magnet, HU80 (80 mm period) undulator was used. The inner-valence photoelectron spectra (PES) were recorded using a 30° wide angle lens VG-Scienta R4000 electron energy analyzer installed on the C-branch of the beamline.[17] The electron energy analyzer's detection axis is perpendicular to the plane of the propagation direction of the SR. To access the angular information on the emitted photoelectrons, the PES were recorded using two linear polarizations of the SR, parallel and perpendicular, meaning that the angle between the SR polarization vector and the electron detection axis is 0° and 90°, respectively. In order to define a photoionization asymmetry parameter β, the 0° and 90° spectra were normalized with respect to photon flux, sample pressure at the interaction region, and data acquisition duration.

PES were measured using a photon energy of 100 eV, with a monochromator exit slit of 150 μm, and a varied groove depth and line spacing plane grating with 2400 lines/mm.[18] For these conditions, the photon bandwidth was estimated to be 8.5 meV fwhm. The electron energy analyzer has been operated at a pass energy of 20 eV with a curved entrance slit of 0.2 mm, thus contributing to the experimental broadening with 10 meV. The largest contribution to the spectral line width is the translational Doppler broadening, estimated to be 17.4 meV in this room temperature measurement.[19] There is also an additional contribution from the rotational Doppler broadening,[20] more difficult to estimate in general due to its strong angular dependence.[21] The total instrumental photoelectron line broadening is about 25 meV without taking into account the rotational Doppler broadening. The binding energy scale was calibrated setting the binding energy of the ν = 0 vibrational substate of the L sequence to 29.76 eV.[8]

HCl sample gas was obtained from AirLiquide and had a stated purity of 99.997%. The vapor pressure in the differentially pumped gas cell by VG-Scienta was estimated to be on the order of 10^{-3} mbar (whereas the measured pressure in the spectrometer vacuum chamber, outside the gas cell, was 8×10^{-6} mbar). The gas cell is equipped with a series of electrodes in order to minimize the effect of plasma potentials caused by the ion density gradient created along the SR propagation axis.

COMPUTATIONAL SECTION

The *ab initio* electronic structure calculations were carried out using the MOLPRO program package[22] in the C_{2v} symmetry point group, where the B_1 and B_2 irreducible representations were equivalently treated. The chlorine and hydrogen atoms were described by a large basis set of aug-cc-pV5Z quality.[23,24] In addition, the basis set of chlorine was augmented by three *s* (exponents: 0.018, 0.00687, 0.002211) and two *p* (exponents: 0.0109, 0.0032) diffuse Gaussian type orbitals (GTOs) and that of hydrogen by two *s* (exponents: 0.0058, 0.0016) and one *p* (exponent: 0.0208) diffuse GTOs.

The calculations were performed using the Complete Active Space Self Consistent Field (CASSCF)[25,26] technique, followed by the internally contracted Multi Reference Configuration Interaction (MRCI)[27,28] approach. In CASSCF, the active space consisted of valence molecular orbitals (MOs) of HCl, to which two σ and two π MOs were added for better relaxation of the wave functions of HCl^+. All valence electrons were correlated. The electronic states having the same spin and space irreducible representation in the C_{2v} point group were averaged together using the CASSCF state-averaged procedure as implemented in MOLPRO. Five $^2\Sigma^+$, three $^2\Sigma^-$, five $^2\Pi$, three $^2\Delta$, and one $^2\Phi$ state were calculated, thus more than 1400 configuration state functions (CSFs) per symmetry were considered. In MRCI, all CASSCF CSFs were taken as reference. This results in more than 25 × 106 uncontracted CSFs per C_{2v} symmetry to be treated.

An active space larger than the valence and a diffuse basis set were used in order to properly describe any possible Rydberg character of the electronic states involved. This treatment describes correctly the highly excited electronic states of HCl^+ without deteriorating the electronic states possessing strictly a valence character, as was recently discussed for N_2 molecule.[29−32] Afterward, these highly correlated wave functions were used to evaluate the spin−orbit coupling matrix elements in Cartesian coordinates. The CASSCF wave functions served as the multielectron basis for the two-step spin−orbit coupling calculations[33,34] at the level of Breit-Pauli Hamiltonian.[35]

The nuclear motion problem was solved using the method of Cooley.[36] The spectroscopic constants discussed below were obtained using the derivatives at the minimum energy distances and standard perturbation theory.

RESULTS

Potential Energy Curves and Spectroscopy. Figure 1 illustrates the evolution along the H−Cl internuclear distance of the potential energy curves of the electronic states of HCl^+ up to 33 eV. These potentials are shown on a relative energy scale with respect to the minimum energy of the ground state (GS) of the neutral molecule. Table 1 lists the spectroscopic constants of the bound electronic states of HCl^+ (see Figure 1).

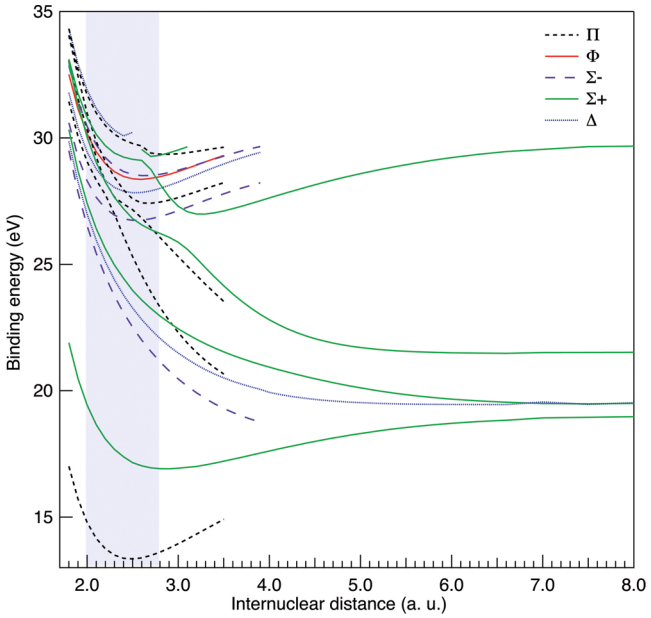

Figure 1. MRCI potential energy curves of the doublet electronic states of HCl^+. The potentials are shown in energy with respect to the minimum energy of HCl^+ ground state potential energy curve. Shaded area shows the FC region.

Table 1. Equilibrium Distances, Harmonic Wavenumbers (ω_e), Anharmonic Terms ($\omega_e\chi_e$), Rotational Constants (B_e and α_e), and the Spin-Orbit Constant at Equilibrium (A_{SO}) for Some Electronic States of HCl^+

state	ω_e (cm^{-1})	$\omega_e\chi_e$ (cm^{-1})	r_e (Å)	B_e (cm^{-1})	A_{SO} (cm^{-1})
$X^2\Pi$	2702.6	61.3	1.3165	9.929	−572.46
					−629.71[a]
	2673.7[d]	54.523[b]	1.315[d]	9.9566[c]	−648.13[c]
$1^2\Sigma^+$	1612.2	38.8	1.5129	7.518	
	1606.5[d]	40.3[d]	1.514[d]	7.505[c,d]	
$2^2\Sigma^-$	2344.6	66.9	1.3460	9.499	
$3^2\Sigma^-$	2156.7	58.8	1.3945	8.849	
$2^2\Delta$	2486.3	66.6	1.3386	9.604	−2.41
					−2.65[a]
$1^2\Phi$	2320.0	55.6	1.3642	9.247	2.74
					3.01[a]

[a]Best estimate of the spin−orbit constant at equilibrium by adding 10% to the ab initio computed values. [b]$X^2\Pi_{3/2}$ state from ref 39. [c]Reference 40. [d]Reference 41.

The ground state, of $X^2\Pi$ space symmetry, is followed by the $A^2\Sigma^+$ and then by six repulsive states in the molecular region accessible from the GS, namely $1^2\Sigma^-$, $1^2\Delta$, $2^2\Pi$, $2^2\Sigma^+$, $3^2\Pi$, and $3^2\Sigma^+$. Some of them present polarization minima at large internuclear distances, such as the $3^2\Sigma^+$. For these states, our present findings agree well with the earlier computations of Pradhan et al.[37] and of Gurin et al.[38] Table 1 lists the spectroscopic parameters of the X and A states of HCl^+. They compare favorably to the experimental values from refs 39−41. For instance, the ω_e values have deviations that do not exceed 1%. This attests to the quality of the predictive data we compute for the upper electronic states (see below).

For energies higher than 26 eV, a series of bound states is found. Most of them were never predicted to exist before. In addition, this work completes the previous theoretical studies,[37,38] allowing a better description for those already known. Generally, these electronic states present potential wells, which are located in the Franck−Condon region accessible by HCl ($X^1\Sigma^+$) photoionization (equilibrium internuclear distance 2.409 a_0 where a_0 = 0.5292 Å[42]), so that they are expected a priori to contribute to the experimental spectrum.

As far as we know, the Φ state has not been calculated before. Its wave function is dominantly described by the $(4\sigma)^2$ $(5\sigma)^2$ $(2\pi)^2$ $(3\pi)^1$ electron configuration. Von Niessen et al.[43] found one state corresponding to our states $1^2\Phi$ and $3^2\Sigma^-$ with leading configuration of type $(2\pi)^{-2}(n\sigma)$ and for the energies 29.5−30.5 eV corresponding to now calculated states of $^2\Pi$ and $^2\Delta$ symmetry they found three states with configurations of type $(5\sigma)^{-2}(n\sigma)$, $(2\pi)^{-2}(n\delta)$.

Angularly Resolved Photoelectron Spectra. Figure 2 illustrates the normalized photoelectron spectra measured at 0° and 90° with respect to the linear polarization of the synchrotron light. The measurement exhibits a very strong and diverse angular dependence of the photoelectron spectrum throughout the considered binding energy range: for some states, such as the rather broad low intensity peak at 29.17 eV, the angular dependence is almost absent (almost no intensity difference), but the situation is exactly opposite for other energy ranges, such as for the strong and broad spectral feature observed in the 0° spectrum around 28.57 eV, which almost completely vanishes in the 90° spectrum.

To gain further insight into the interpretation of these puzzling observations, an estimation of the photoelectron asymmetry parameter β is also plotted in Figure 2 as a function of the binding energy, as obtained using the formula

$$\beta = 2[I_{0^\circ}/I_{90^\circ} - 1]/[I_{0^\circ}/I_{90^\circ} + 2] \quad (1)$$

where I_θ (θ = 0°, 90°) is the angularly resolved spectrum recorded at the angle θ. Here, the β parameter is used as an additional tool to identify the transitions toward the same final electronic state. This assumes that β is independent of the vibrational substate for a given electronic state, which, as discussed above, is known to be an inaccurate approximation in case of resonant photoemission processes,[14,15] as well as just above the photoionization threshold.[13] However, this approximation should be valid at the present photon energy of 100 eV, which was chosen to avoid any resonant electronic transitions embedded in the photoionization continuum. Since the measured inner-valence spectra consist of numerous overlapping transitions, some of which are broad bands associated with dissociative final states (see below), the absolute values of β shown in Figure 2 should be taken with precaution, when ascribing them to a specific state. The labeling of the states in Figure 2 follows the nomenclature in ref 8. However, we suggest a different interpretation for a few states, and the *ab initio* calculations allowed us to provide an exact assignment for most of the states. The comparison between our current experimental data, the previous experimental results from ref 8, and the present theoretical results is presented in Table 2.

DISCUSSION

Figure 3 illustrates the aligned potential energy curves (shifted by +0.54 eV) and the experimental spectra. The studied

dx.doi.org/10.1021/jp504505e | J. Phys. Chem. A 2014, 118, 4975−4981

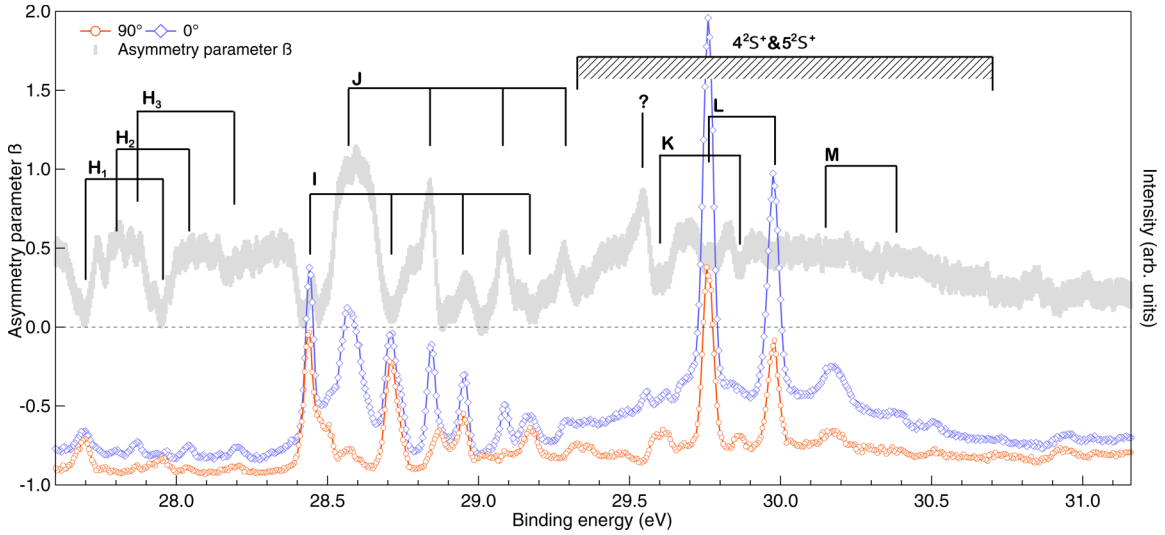

Figure 2. Experimental inner-valence PES of HCl measured at 0° (blue line with diamonds) and 90° (red line with circles) between the electron detection axis and the polarization vector of the 100 eV synchrotron light. The asymmetry parameter β (gray line with error bars) is also shown to better distinguish spectral features originating from the transitions to the same electronic state. Labeling follows the nomenclature of Burmeister et al.,[8] but some of the observed structures are reinterpreted (see text for details).

Table 2. Experimental and Theoretical Vertical Ionization Energies Determined for the Studied Vibronic States of HCl^+ in the Binding Energy Range 27.5−30.5 eV[e]

			energy (eV)		
state	label	ν	exp.	ref 8	theory[a]
$2^2\Sigma^-$	H_1	0	*b*	27.12	26.82
		1	*b*	27.42	27.10
		2	27.69	27.67	27.35
		3	27.94		27.60
		4	28.14		27.82
$4^2\Pi$	H_2	0	27.80	27.77	~27.5[d]
		1	28.04	28.02	
$2^2\Delta$	H_3	0	27.87	27.93	27.93
		1	28.20	28.19	28.22
$1^2\Phi$	I	0	28.44	28.43	28.44
		1	28.72	28.69	28.71
		2	28.96	28.95	28.97
		3	29.17	29.17	29.22
$3^2\Sigma^-$	J	0	28.58	28.56	28.58
		1	28.84	28.85	28.83
		2	29.09	29.08	29.07
		3	29.29	29.34	29.30
$4^2\Sigma^-$?		0	29.56		
$5^2\Pi$?	K	0	29.59	29.62	~29.4[d]
		1	29.85	29.87	
$^2\Pi$?	L	0	29.76	29.76	~29.5[d]
		1	29.98	29.98	
		2	*c*	30.17	
$3^2\Delta$	M	0	30.18		~30.2[d]
		1	30.37		

[a]0.54 eV was added to all the calculated energy values. [b]These transitions are out of the studied energy range. [c]Interpreted to be a transition to $3^2\Delta$, ν = 0. [d]Since spectroscopic constants ω_e and $\omega_e\chi_e$ were not calculated for these states, the position of the first vibrational level is approximate. [e]The estimated error limits for the present measurement are ±0.03 eV.

binding energy region 27.5−30.5 eV exhibits several interesting phenomena, which are discussed below.

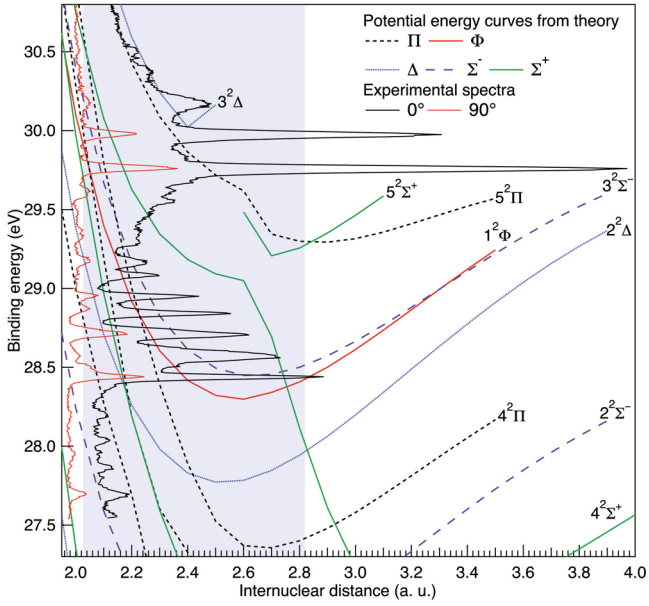

Figure 3. Comparison between experimental spectra measured with different light polarizations and the calculated potential energy curves. PECs have been shifted by 0.54 eV. The shaded area shows the FC region.

By just looking at the potential energy curves one could expect strong transitions to take place from the GS to the $2^2\Delta$ ionic state. This state consists of configurations $(4\sigma)^2(5\sigma)^2(2\pi)^2(6\sigma)^0(7\sigma)^1$ (90%), $(4\sigma)^2(5\sigma)^2(2\pi)^2(6\sigma)^1$ (7%), and $(4\sigma)^2(5\sigma)^0(2\pi)^2(6\sigma)^2(7\sigma)^1$ (0.5%). Near the equilibrium internuclear distance, the ground state of neutral HCl consists mainly of the $(4\sigma)^2(5\sigma)^2(2\pi)^4(6\sigma)^0$ configuration,[44] so it can be easily understood that the transition matrix element between the GS and the $2^2\Delta$ state is small, since it requires a shakeup transition to the 7σ orbital. Very weak peaks matching the vibrational sublevels of this state are observed in the experimental spectrum, so it can be tentatively concluded that these peaks (H_3 progression in Figure 2) correspond to weak transitions to the $2^2\Delta$ state. Finally, the sequences H_1 and

dx.doi.org/10.1021/jp504505e | J. Phys. Chem. A 2014, 118, 4975−4981

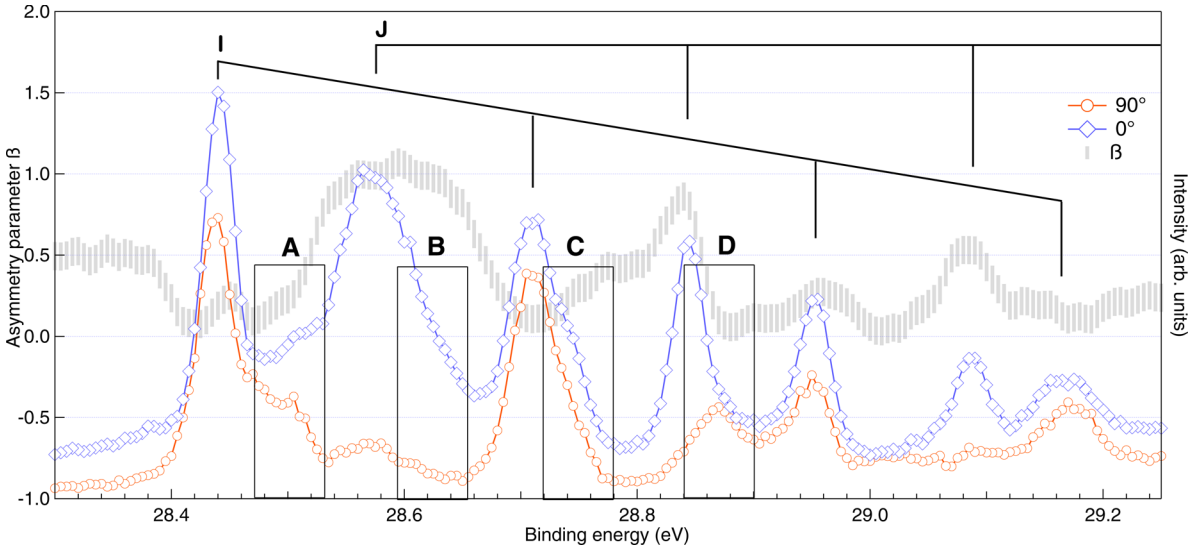

Figure 4. Zoom of the photoelectron spectra of I and J sequences presented in 2. Rectangles A, B, C, and D indicate regions where we suspect to see hints of the underlying transitions or phenomena unexplainable at this level of theory. See text for details.

H_2 can be tentatively assigned to the $2^2\Sigma^-$ and $4^2\Pi$ states, respectively. The correspondence in energy is not very good, but the vibrational spacing is well-matched for the $2^2\Sigma^-$ state.

The most striking phenomenon is an almost complete suppression of the J-state vibrational progression (Figure 2), when the spectrum is measured with the perpendicular (90°) polarization of the SR. Based on the theoretical results (see Figure 3 and Table 2) the vibrational progressions I and J can be assigned to the electronic states $1^2\Phi$ and $3^2\Sigma^-$, respectively. The approximate β parameter in Figure 2 differs significantly between the vibrational substates within the $3^2\Sigma^-$ state (progression J), the higher excited vibrational substates having smaller β values. As the used photon energy is about 70 eV above the ionization thresholds of the studied states, we can exclude a non-Franck−Condon vibrational dependence of the asymmetry parameter due to continuum resonances.[45] The spectra in the energy region of I and J progressions are not completely "clean"; it seems like there are underlying structures present. Figure 4 indicates, as an example, four regions which are not easily explainable by considering only simple Franck−Condon overlaps to the $1^2\Phi$ and $3^2\Sigma^-$ states. The 90° spectrum shows a clear tail of the $1^2\Phi\nu = 0$ peak (indicated with A in Figure 4), and furthermore, the $\nu = 1$ peak is broader than the $\nu = 0$ peak of the sequence and also clearly asymmetric (indicated with C in Figure 4). Moreover, the first peak of the J progression ($3^2\Sigma^-\nu = 0$) is remarkably broader (about 3 times larger fwhm value) than the other peaks belonging to either the I or the J progressions and asymmetric to the higher binding energy side (indicated with B in Figure 4). The maximum of the $3^2\Sigma^-$ $\nu = 1$ peak (indicated with D in Figure 4) is clearly displaced in the 90° spectrum compared to the 0° spectrum.

These kinds of peak broadenings and asymmetries could be related to the rotational heating of the molecule due to the rotational Doppler effect.[21] A recent work by Miron et al.[46] confirms experimentally the existence of a rotational Doppler effect in the case of the $A^2\Sigma^+$ state of the HCl cation. This study also reveals a decreasing rotational Doppler broadening for the vibrationally resolved differential photoionization cross section with increasing vibrational quantum number ν, due to the strong sensitivity of the effect to the bond length. According to the calculations by von Niessen et al.,[43] the Σ symmetry state in this energy region still has significant contribution from the configurations $4\sigma^{-1}$ and $5\sigma^{-1}$, which can be assumed to be affected by the rotational Doppler broadening due to the significant H 1s atomic orbital contribution to these molecular orbitals. Thus, it is reasonable to assume that some of the asymmetrical broadening observed here can be due to the rotational Doppler effect, but the effect seen for example in the case of the $3^2\Sigma^-\nu = 0$ peak is way too large to be explained solely by the rotational heating of the molecule. Moreover, the observed energy shift of 25 meV of the $3^2\Sigma^-\nu = 1$ peak is also by far too large to be explained by the rotational Doppler effect, which would be surprising to see for only a selected vibrational peak. Furthermore, the almost distinguishable peak accompanying the $1^2\Phi\nu = 0$ peak cannot be explained by the rotational Doppler effect. These facts suggest that there are more transitions involved to this spectral region than only the ones related to the $1^2\Phi$ and $3^2\Sigma^-$ states. As seen in Figure 1, the $4^2\Sigma^+$ state is actually the bound counterpart of the avoided crossing with the $3^2\Sigma^+$ state, and thus the $4^2\Sigma^+$ is not dissociative but could be responsible for underlying structures observed via the population of highly excited vibrational states. The dissociation limit of the $4^2\Sigma^+$ is 28.86 eV ($H + Cl^{+*}(3s3p^6\ ^3P)$).[44] A plausible explanation for the broadening of the $3^2\Sigma^-\nu = 0$ band could be spin−orbit induced predissociation. However, we calculated a predissociation rate of about $3.4 \times 10^{10}\ s^{-1}$, which implies a full-width-at-half-maximum (Γ) of only 22 μeV i.e. orders of magnitude smaller than the currently observed line broadening. While state-of-the-art methodologies were used for our computations, they still cannot properly describe this rich photoionization dynamics, applying either diabatic or adiabatic models. We believe that a more complex method, where time and energy couplings are calculated in the same framework, might be needed.

The broad band starting from 29.3 eV and particularly enhanced in the 0° measurement is due to the dissociation continuum accessible through the avoided crossing of the $4^2\Sigma^+$ and $5^2\Sigma^+$ states. In the 90° spectrum there is a weak peak at 29.6 eV, which is absent in the 0° spectrum, and marked with a question mark in Figure 2. This could be a transition to the bound $5^2\Sigma^+$ state. Possibly also the low binding energy shoulder of the first peak of the L progression could belong to the same

dx.doi.org/10.1021/jp504505e | J. Phys. Chem. A 2014, 118, 4975−4981

$5^2\Sigma^+$ electronic state. The K progression can be due to the population of the first vibrational levels of the $5^2\Pi$ state. Around 29.8 and 30.0 eV two very intense transitions are observed (progression L in Figure 2). These states are believed to be of Π symmetry. However, the shape of the potential energy curve suggests that there is an avoided crossing with an upper Π state. Above these strong lines, a somewhat broader structure is observed, which has been previously assigned to also belong to the L progression. We propose here a new assignment of this spectral feature, as being due to the transition to the $3^2\Delta,\nu = 0$ state, labeled as M in Figure 2. This line is considerably broader compared to the strong lines just below it. This broadening is caused by spin−orbit induced predissociation.

CONCLUSION

In this study we achieved the observation and the satisfactory interpretation of the angularly resolved inner-valence photoelectron spectrum of hydrogen chloride using state-of-the-art experimental and theoretical tools, adding new insights to previous theoretical and experimental works. The asymmetry parameter β turned out to be a useful tool to distinguish several overlapping vibrational sequences. In addition, the studied inner-valence region with strong electron correlation effects exhibits a series of phenomena. We were able to confirm or to propose new assignments for most of the observed vibronic transitions. Moreover, we observe a significant broadening of the first vibrational substate of the $3^2\Sigma^-$ state. It may be that the broadening of this state can only be explained by using a full dynamical model where time and energy couplings are calculated in the same framework. Generally, the accurate characterization of molecular Valence-Rydberg states is important since these states play a key role in attophysics, as intermediates, and astrochemistry of hot regions of the interstellar medium (see e.g. refs 47 and 48 and references therein). The present investigations should motivate new theoretical and experimental developments, as for instance using time-resolved photoionization measurements to fully characterize this important class of molecular states.

AUTHOR INFORMATION

Corresponding Authors

*E-mail: majdi.hochlaf@univ-mlv.fr.
*E-mail: Catalin.Miron@synchrotron-soleil.fr.

Notes

The authors declare no competing financial interest.

ACKNOWLEDGMENTS

Data collection was performed at the PLEIADES beamline at the SOLEIL Synchrotron, France (proposal no. 20110708). We are grateful to E. Robert for technical assistance and to the SOLEIL staff for stable operation of the equipment and storage ring during the experiments. C.M. and J.H.D.B. acknowledge financial support from The France-Stanford Center for Interdisciplinary Studies. We acknowledge support from the European COST actions CM1204 - XUV/X-ray light and CM1002 CODECS and fast ions for ultrafast chemistry (XLIC). G.S. acknowledges the support from the Brazilian funding agency CAPES (8683-11-5) for scholarship grant.

REFERENCES

(1) Solomon, S.; Garcia, R. R.; Rowland, F. S.; Wuebbels, D. J. On the depletion of Antarctic ozone. *Nature* **1986**, *321*, 755−758.
(2) De Luca, M.; Gupta, H.; Neufeld, D.; Gerin, M.; Teyssier, D.; Drouin, B. J.; Pearson, J. C.; Lis, D. C.; Monje, R.; Phillips, T. G.; et al. Herschel/HIFI discovery of HCl^+ in the interstellar medium. *Astrophys. J. Lett.* **2012**, *751*, L37.
(3) Morin, P.; Miron, C. Ultrafast dissociation: An unexpected tool for probing molecular dynamics. *J. Electron. Spec. Relat. Phenom.* **2012**, *185*, 259−266.
(4) Aksela, H.; Aksela, S.; Ala-Korpela, M.; Sairanen, O.-P.; Hotokka, M.; Bancroft, G. M.; Tan, K. H.; Tulkki, J. Decay channels of core-excited HCl. *Phys. Rev. A* **1990**, *41*, 6000−6005.
(5) Feifel, R.; Burmeister, F.; Sałek, P.; Piancastelli, M. N.; Bässler, M.; Sorensen, S. L.; Miron, C.; Wang, H.; Hjelte, I.; Björneholm, O.; et al. Observation of a continuum-continuum interference hole in ultrafast dissociating core-excited molecules. *Phys. Rev. Lett.* **2000**, *85*, 3133−3136.
(6) Kavčič, M.; Žitnik, M.; Bučar, K.; Mihelič, A.; Carniato, S.; Journel, L.; Guillemin, R.; Simon, M. Electronic state interferences in resonant x-ray emission after K-shell excitation in HCl. *Phys. Rev. Lett.* **2010**, *105*, 113004.
(7) Burmeister, F.; Sorensen, S. L.; Björneholm, O.; Naves de Brito, A.; Fink, R. F.; Feifel, R.; Hjelte, I.; Wiesner, K.; Giertz, A.; Bässler.; et al. Nonadiabatic effects in photoelectron spectra of HCl and DCl. I. Experiment. *Phys. Rev. A* **2001**, *65*, 012704.
(8) Burmeister, F.; Andersson, L. M.; Öhrwall, G.; Richter, T.; Zimmermann, P.; Godehusen, K.; Martins, M.; Karlsson, H. O.; Sorensen, S. L.; Björneholm, O.; et al. A study of the inner-valence ionization region in HCl and DCl. *J. Phys. B: At., Mol. Opt. Phys.* **2004**, *37*, 1173−1183.
(9) Akagi, H.; Otobe, T.; Staudte, A.; Shiner, A.; Turner, F.; Dörner, R.; Villeneuve, D. M.; Corkum, P. B. Laser tunnel ionization from multiple orbitals in HCl. *Science* **2009**, *325*, 1364−1367.
(10) Adam, M. Y. Highly resolved photoelectron spectra of the HCl inner valence shell. *Chem. Phys. Lett.* **1986**, *128*, 280−286.
(11) Kukk, E.; Wills, A.; Berrah, N.; Langer, B.; Bozek, J. D.; Nayadin, O.; Alsherhi, M.; Farhat, A.; Cubaynes, D. Angle-resolved two-dimensional mapping of electron emission following Cl 2p excitations in the HCl molecule. *Phys. Rev. A* **1998**, *57*, R1485−R1488.
(12) Mistrov, D. A.; De Fanis, A.; Kitajima, M.; Hoshino, M.; Shindo, H.; Tanaka, T.; Tamenori, Y.; Tanaka, H.; Pavlychev, A. A.; Ueda, K. Vibrational effects on the shape resonance energy in the K-shell photoionization spectra of CO. *Phys. Rev. A* **2003**, *68*, 022508.
(13) Lucchese, R. R.; Söderström, J.; Tanaka, T.; Hoshino, M.; Kitajima, M.; Tanaka, H.; De Fanis, A.; Rubensson, J.-E.; Ueda, K. Vibrationally resolved partial cross sections and asymmetry parameters for nitrogen K-shell photoionization of the N_2O molecule. *Phys. Rev. A* **2007**, *76*, 012506.
(14) Miron, C.; Kimberg, V.; Morin, P.; Nicolas, C.; Kosugi, N.; Gavrilyuk, S.; Gel'mukhanov, F. Vibrational scattering anisotropy generated by multichannel quantum interference. *Phys. Rev. Lett.* **2010**, *105*, 093002.
(15) Lindblad, A.; Kimberg, V.; Söderström, J.; Nicolas, C.; Travnikova, O.; Kosugi, N.; Gel'mukhanov, F.; Miron, C. Vibrational scattering anisotropy in O_2 − dynamics beyond the Born − Oppenheimer approximation. *New J. Phys.* **2012**, *14*, 113018.
(16) Travnikova, O.; Liu, J. C.; Lindblad, A.; Nicolas, C.; Söderström, J.; Kimberg, V.; Gel'mukhanov, F.; Miron, C. Circularly polarized x-rays: Another probe of ultrafast molecular decay dynamics. *Phys. Rev. Lett.* **2010**, *105*, 233001.
(17) Söderström, J.; Lindblad, A.; Grum-Grzhimailo, A.; Travnikova, O.; Nicolas, C.; Svensson, S.; Miron, C. Angle-resolved electron spectroscopy of the resonant Auger decay in xenon with meV energy resolution. *New J. Phys.* **2011**, *13*, 073014.
(18) Miron, C.; Nicolas, C.; Travnikova, O.; Morin, P.; Sun, Y. P.; Gel'mukhanov, F.; Kosugi, N.; Kimberg, V. Imaging molecular potentials using ultrahigh-resolution resonant photoemission. *Nat. Phys.* **2012**, *8*, 135−138.

(19) Baltzer, P.; Karlsson, L.; Lundqvist, M.; Wannberg, B. V. Resolution and signal − to − background enhancement in gas − phase electron spectroscopy. *Rev. Sci. Instrum.* **1993**, *64*, 2179−2189.
(20) Thomas, T. D.; Kukk, E.; Ueda, K.; Ouchi, T.; Sakai, K.; Carroll, T. X.; Nicolas, C.; Travnikova, O.; Miron, C. Experimental observation of rotational doppler broadening in a molecular system. *Phys. Rev. Lett.* **2011**, *106*, 193009.
(21) Sun, Y.-P.; Wang, C.-K.; Gel'mukhanov, F. Rotational Doppler effect in x−ray photoionization. *Phys. Rev. A* **2010**, *82*, 052506.
(22) MOLPRO is a package of ab initio programs written by Werner, H.-J.; Knowles, P. J.; Knizia, G.; Manby, F. R.; Schütz, M.; Celani, P.; Korona, T.; Lindh, R.; Mitrushenkov, A.; Rauhut, G.; Shamasundar, K. R.; et al. See http://www.molpro.net for more details.
(23) Woon, D. E.; Dunning, T. H., Jr. Gaussian basis sets for use in correlated molecular calculations. III. The atoms aluminum through argon. *J. Chem. Phys.* **1993**, *98*, 1358−1371.
(24) Kendall, R. A.; Dunning, T. H., Jr.; Harrison, R. J. Electron affinities of the first-row atoms revisited. Systematic basis sets and wave functions. *J. Chem. Phys.* **1992**, *96*, 6796−6806.
(25) Knowles, P. J.; Werner, H.-J. An efficient second−order MC SCF method for long configuration expansions. *Chem. Phys. Lett.* **1985**, *115*, 259−267.
(26) Werner, H.-J.; Knowles, P. J. A second order multiconfiguration SCF procedure with optimum convergence. *J. Chem. Phys.* **1985**, *82*, 5053−5063.
(27) Knowles, P. J.; Werner, H.-J. An efficient method for the evaluation of coupling coefficients in configuration interaction calculations. *Chem. Phys. Lett.* **1988**, *145*, 514−522.
(28) Werner, H.-J.; Knowles, P. J. An efficient internally contracted multiconfiguration-reference configuration interaction method. *J. Chem. Phys.* **1988**, *89*, 5803−5814.
(29) Spelsberg, D.; Meyer, W. Dipole−allowed excited states of N_2: Potential energy curves, vibrational analysis, and absorption intensities. *J. Chem. Phys.* **2001**, *115*, 6438−6449.
(30) Ndome, H.; Hochlaf, M.; Lewis, B. R.; Heays, A. N.; Gibson, S. T.; Lefebvre-Brion, H. Sign reversal of the spin-orbit constant for the $C^3\Pi_u$ state of N_2. *J. Chem. Phys.* **2008**, *129*, 164307.
(31) Hochlaf, M.; Ndome, H.; Hammoutène, D. Quintet electronic states of N_2. *J. Chem. Phys.* **2010**, *132*, 104310.
(32) Hochlaf, M.; Ndome, H.; Hammoutène, D.; Vervloet, M. Valence-Rydberg electronic states of N_2: spectroscopy and spin-orbit couplings. *J. Phys. B: At., Mol. Opt. Phys.* **2010**, *43*, 245101.
(33) Llusar, R.; Casarrubios, M.; Barandiarán, Z.; Seijo, L. Ab initio model potential calculations on the electronic spectrum of Ni^{2+}−doped MgO including correlation, spin-orbit and embedding effects. *J. Chem. Phys.* **1996**, *105*, 5321−5330.
(34) Zeng, T.; Fedorov, D. G.; Schmidt, M. W.; Klobukowski, M. Two-component natural spinors from two-step spin-orbit coupled wave functions. *J. Chem. Phys.* **2011**, *134*, 214107.
(35) Schweizer, M.; Werner, H.-J.; Knowles, P. J.; Palmieri, P. Spin-orbit matrix elements for internally contracted multireference configuration interaction wavefunctions. *Mol. Phys.* **2000**, *98*, 1823−1833.
(36) Cooley, J. W. An improved eigenvalue corrector formula for solving the Schrödinger equation for central fields. *Math. Comput.* **1961**, *15*, 363−374.
(37) Pradhan, A. D.; Kirby, K. P.; Dalgarno, A. Theoretical study of HCl^+ Potential curves, radiative lifetimes, and photodissociation cross sections. *J. Chem. Phys.* **1991**, *95*, 9009−9023. Pradhan, A. D.; Kirby, K. P.; Dalgarno, A. Erratum: Theoretical study of HCl^+: Potential curves, radiative lifetimes, and photodissociation cross sections. *J. Chem. Phys.* **1995**, *103*, 864−864.
(38) Gurin, V. S.; Korolkov, M. V.; Matulis, V. E.; Rakhmanov, S. K. Symmetry-adapted-cluster configuration interaction study of the doublet states of HCl^+: Potential energy curves, dipole moments, and transition dipole moments. *J. Chem. Phys.* **2007**, *126*, 124321.
(39) Yencha, A. J.; Cormack, A. J.; Donovan, R. J.; Hopkirk, A.; King, G. C. Threshold photoelectron spectroscopy of HCl and DCl. *Chem. Phys.* **1998**, *238*, 109−131.
(40) Saenger, K. L.; Zare, R. N.; Mathews, C. W. A reexamination of the spin-rotation constant for $^2\Pi$ states: The A-X band system of HCl^+. *J. Mol. Spectrosc.* **1976**, *61*, 216−230.
(41) Sheasley, W. D.; Mathews, C. W. The emission spectra of $H^{35}Cl^+$, $H^{37}Cl^+$, $D^{35}Cl^+$, and $D^{37}Cl^+$ in the region 2700−4100 Å. *J. Mol. Spectrosc.* **1973**, *47*, 420−439.
(42) Huber, K. P.; Herzberg, G. *Molecular Spectra And Constants Of Diatomic Molecules*; Van Nostrand Reinhold: New York, 1979.
(43) von Niessen, W.; Tomasello, P.; Schirmer, J.; Cederbaum, L. S.; Cambi, R.; Tarantelli, F.; Smagellotti, A. Valence ionization of HCl. An investigation of many-body effects. *J. Chem. Phys.* **1990**, *92*, 4331−4341.
(44) Hiyama, M.; Iwata, S. Assignment of the photoelectron spectrum of HCl above 20 eV. *Chem. Phys. Lett.* **1993**, *210*, 187−192.
(45) Parr, A. C.; Ederer, D. L.; West, J. B.; Holland, D. M. P.; Dehmer, J. L. Triply differential photoelectron studies of non-Franck-Condon behavior in the photoionization of acetylene. *J. Chem. Phys.* **1982**, *76*, 4349−4355.
(46) Miron, C.; Miao, Q.; Nicolas, C.; Bozek, J. D.; Andrałojć, W.; Patanen, M.; Simões, G.; Travnikova, O.; Ågren, H.; Gel'mukhanov, F. Site-selective photoemission from delocalised valence shells: the role of molecular rotation. *Nat. Commun.* **2014**, *5*, 3816. DOI: 10.1038/ncomms4816.
(47) Reisler, H.; Krylov, A. I. Interacting Rydberg and valence states in radicals and molecules: experimental and theoretical studies. *Int. Rev. Phys. Chem.* **2009**, *28*, 267−308.
(48) Lucchini, M.; Kim, K.; Calegari, F.; Kelkensberg, F.; Siu, W.; Sansone, G.; Vrakking, M. J. J.; Hochlaf, M.; Nisoli, M. Autoionization and ultrafast relaxation dynamics of highly excited states in N_2. *Phys. Rev. A* **2012**, *86*, 043404.